European Review for Medical and Pharmacological Sciences 2021; 25: 335-343

# Inhibition of microRNA-495 inhibits hypoxia-induced apoptosis in H9c2 cells *via* targeting NFIB

W.-Q. ZHANG[1], L. FENG[2], H.-J. WANG[3], X.-F. DU[1], X.-L. HAO[1], Y.-Z. LI[1], L. CHENG[4]

[1]Department of Critical Care Medicine, Yantai Affiliated Hospital of Binzhou Medical University, Yantai, China
[2]Department of Pharmacy, Yantai Affiliated Hospital of Binzhou Medical University, Yantai, China
[3]Department of Thoracic Surgery, Yantai Affiliated Hospital of Binzhou Medical University, Yantai, China
[4]Department of Cardiology, Yantai Affiliated Hospital of Binzhou Medical University, Yantai, China

**Abstract. – OBJECTIVE: Acute myocardial infarction (AMI) is a serious cardiovascular disease that threatens human life. MicroRNA is considered to be an important participant in the pathophysiology of AMI. This article focused on the role of microRNA-495 (miR-495) in regulating apoptosis after myocardial infarction (MI) and its underlying mechanisms.**

**MATERIALS AND METHODS: H9c2 cells were cultured in an incubator containing 1% O2 to establish a cell model of MI. Quantitative reverse-transcription polymerase chain reaction (RT-PCR) was utilized to detect miR-495 expression in H9c2 cells. The effects of miR-495 and NFIB on hypoxia-treated H9c2 cells were observed by Western blot, lactate dehydrogenase (LDH) detection, MTT (3-(4,5-dimethylthiazol-2-yl)-2,5-diphenyl tetrazolium bromide) assay, flow cytometry, and terminal dexynucleotidyl transferase(TdT)-mediated dUTP nick end labeling (TUNEL) staining. Luciferase reporter gene experiment was used to prove the regulatory relationship between miR-495 and NFIB.**

**RESULTS: Hypoxia induced injury to H9c2 cells, which was manifested by decreased cell viability, increased LDH release, increased pro-apoptotic proteins (Bax, Cleaved Caspase-3) expression, decreased anti-apoptotic protein (Bcl-2) expression, and increased in the rate of apoptosis and TUNEL positive cells. MiR-495 expression was remarkably increased in H9c2 cells treated with hypoxia. Inhibiting miR-495 expression markedly alleviated the hypoxia-induced injury in H9c2 cells, while silencing NFIB aggravated the hypoxia-induced damage. In addition, NFIB was confirmed to be the target of miR-495.**

**CONCLUSIONS: MiR-495 expression was increased in hypoxia-treated H9c2 cells. Silencing miR-495 could significantly inhibit hypoxia-induced apoptosis of H9c2 cells by targeting NFIB.**

*Key Words:*
Acute myocardial infarction, MicroRNA-495, Apoptosis, NFIB.

## Introduction

AMI is a rapid and persistent phenomenon of hypoxia and ischemia in coronary arteries due to human or non-human factors, which eventually leads to myocardial necrosis. It is one of the most common emergency diseases in clinical practice. Due to its high mortality rate and poor prognosis, AMI has posed a serious threat to people's health[1]. At present, the treatment of myocardial infarction is diversified, mainly including drug therapy, coronary artery bypass and interventional therapy[2-4]. Although these conventional treatments relieve the patient's pain to a certain extent, they cannot fundamentally recover the damaged myocardium. Therefore, there is an urgent need to find new effective drugs or therapeutic targets to provide new treatment strategies for myocardial infarction.

MicroRNAs (MiRNAs) are a class of highly conserved and non-coding small RNAs with a length of 19-25 ribonucleic acids that regulate gene expression at the post-transcriptional level. They are involved in almost all pathophysiological processes of the heart[5]. MiRNAs are closely involved in the regulation of cardiac

*Corresponding Author:* Lin Cheng, MM; e-mail: chl7619@mail.sdufe.edu.cn

development, cardiac hypertrophy, heart failure and reperfusion injury, and play an important role in the differentiation, growth, proliferation, apoptosis and fibrosis of cardiomyocytes[6-8]. At present, miRNAs that are expressed in myocardial tissues and whose functions and target genes have been verified through experiments include miR-1, miR-21, miR-23a, miR-133, etc. The functions and targets of other miRNAs involved in myocardial physiopathological processes need to be further confirmed. In recent years, miR-495 has been reported to regulate tumor cell apoptosis, proliferation and migration[9]. In addition, Liang et al[10] demonstrated that inhibition of miR-495 could enhance angiogenesis and thus protect the myocardial injury caused by MI. However, the regulation of miR-495 on the apoptosis of myocardial cells after MI is still poorly understood.

In this paper, we constructed a hypoxia-induced H9c2 cell injury model to study the regulatory effects of miR-495 on apoptosis of cardiomyocyte after MI. Our results suggested that miR-495 could be a potential therapeutic target for MI.

## Materials and Methods

### Cell Culture and Transfection

The complete medium required for the growth of H9c2 cells is composed of three components: Dulbecco's Modified Eagle's Medium (DMEM, Rockville, MD, USA), 10% fetal bovine serum (FBS, Invitrogen, Carlsbad, CA, USA), 1% penicillin/streptomycin (Invitrogen, Carlsbad, CA, USA). The cells were cultured at 37°C in a 5% $CO_2$ incubator, and the cell culture medium was changed every 2 days. The cells in the hypoxic treatment group were cultured at 37°C in a constant-temperature cell incubator containing 5% $CO_2$ and 1% $O_2$.

To study the role of miR-495, miR-495 inhibitor or negative control (NC) (RiboBio, Guangzhou, China) was transfected into H9c2 cells using Transfection Kit (RiboBio, Guangzhou, China) according to the protocols. H9c2 cells were divided into control group, hypoxia group, hypoxia+NC group, hypoxia+inhibitor group.

To explore the role of NFIB, small interfering RNA-NFIB (siR-NFIB) or siRNA negative control (siR-NC) (RiboBio, Guangzhou, China) was co-transfected with miR-495 inhibitor into H9c2 cells using Transfection Kit according to the protocols. So H9c2 cells were divided into hypoxia+inhibitor+siR-NC (+siR-NC) group, hypoxia+inhibitor+siR-NFIB (+siR-NFIB) group.

### MTT [3-(4,5-Dimethylthiazol-2-yl)-2,5-Diphenyl Tetrazolium Bromide] Assay

H9c2 cell viability was detected using MTT assay. The cells were transfected with miR-495 inhibitor or NC, followed by hypoxia treatment. After that, 20 μL MTT solution (YEASEN, Shanghai, China) was added into wells for 4 hours at 37°C, and then 150 μL dimethyl sulfoxide (DMSO) solution (Sigma-Aldrich, St. Louis, MO, USA) was added. Finally, the absorbance at 490 nm was detected by a spectrophotometer.

### Lactate Dehydrogenase (LDH) Contents

The supernatant of H9c2 Cells was collected and LDH levels in the cell supernatant were detected using LDH enzyme-linked immunosorbent assay (ELISA) kit (Dojindo Molecular Technologies, Kumamoto, Japan) according to the manufacturer's instructions.

### Western Blot

Protein extraction kit (KeyGen, Shanghai, China) was utilized to extract total protein of H9c2 cells. H9c2 cells were lysed with radioimmunoprecipitation assay (RIPA) lysate containing 1% phenylmethylsulfonyl fluoride (PMSF) (Beyotime, Shanghai, China). After the cells were collected, they were shaken repeatedly to fully lyse, and finally centrifuged at 12000 g for about 5 minutes to collect total protein and remove cell debris. The concentration of the protein samples was measured by bicinchoninic acid assay (BCA) detection kit (KeyGen, Shanghai, China). After that, sodium dodecyl sulphate (SDS) loading buffer (KeyGen, Shanghai, China) was added, and the mixture was denatured by boiling.

According to the molecular weight of the target protein, formulate an appropriate concentration of sodium dodecyl sulphate-polyacrylamide gel electrophoresis (SDS-PAGE) gel. After adding 30 μg of total protein to each lane, electrophoresis was started at a voltage of 70 V. Until bromophenol blue moved to the separation gel, the voltage was increased to 120 V. When bromophenol blue overflowed from the separation gel, electrophoresis was stopped. The polyvinylidene difluoride (PVDF) membrane (Beyotime, Shanghai, China) was activated with alcohol, and then the protein was transferred to the

PVDF membrane at a voltage of 100 V. Then, the non-specific antigen on the protein membranes was blocked by 5% skim milk. Then, the protein membranes were incubated with primary antibodies (Bcl-2, Abcam, Cambridge, MA, USA, Rabbit, 1:1000; Bax, Abcam, Cambridge, MA, USA, Rabbit, 1:1000; Cleaved Caspase-3, Abcam, Cambridge, MA, USA, Rabbit, 1:1000; total Caspase-3, Abcam, Cambridge, MA, USA, Rabbit, 1:1000; NFIB, Abcam, Cambridge, MA, USA, Rabbit, 1:1000; GAPDH, Abcam, Cambridge, MA, USA, Rabbit, 1:1000) overnight. After that, the secondary antibody was used to incubate the protein membranes at room temperature. Finally, the gel imaging system was used to expose the protein membranes.

### Flow Cytometry

H9c2 cells were collected using trypsin digestion followed by centrifugation. Then, H9c2 cells were repeatedly resuspended with phosphate-buffered saline (PBS) and centrifuged to wash the cells. After that, 300 μL of Binding buffer was utilized to resuspend H9c2 cells. 5 μL of Annexin V-FITc (Beyotime, Shanghai, China) and propidium iodide (PI; Beyotime, Shanghai, China) were added to each tube. Finally, the apoptosis rate of cells was analyzed by flow cytometry.

### Quantitative Reverse-Transcription Polymerase Chain Reaction (RT-PCR) Analysis

Total RNA of H9c2 cells was extracted using TRIzol reagent (Invitrogen, Carlsbad, CA, USA). The optical density value at 260 and 280 nm wavelengths were detected to calculate the concentration of total RNA. The miScript RT II kit (Qiagen, Hilden, Germany) was used to synthesize a miRNA cDNA library in accordance with the protocols. The synthesized cDNA was stored at -80°C.

The miScript SYBR Green PCR kit (Qiagen, Hilden, Germany) was used to perform the amplification reaction. 20 μL reaction system: 2 μL of 10 × miScript Universal Primer, 10 μL of 2 × QuantiTect SYBR Green PCR Master Mix, 2 μL of 10 × miScript miR-495 or U6 primer, 5 μL of ribonase-free water, 1 μL of miRNA cDNA template. The relative expression of the genes was calculated using 2-ΔΔCT method. U6 was the internal control of miR-495. All the primers were listed in Table I.

### Terminal Dexynucleotidyl Transferase (TdT)-Mediated dUTP Nick End Labeling (TUNEL) Staining

TUNEL kit (Beyotime, Shanghai, China) was utilized to observe the apoptosis of H9c2 cells as instructed by the manufacturer. And the nucleus was stained with DAPI (Beyotime, Shanghai, China). TUNEL staining was observed by a Confocal Laser Scanning Microscope (CLSM).

### Luciferase Activity Assay

To explore the mechanism of miR-495, luciferase reporter assay was performed. Luciferase reporters (RiboBio, Guangzhou, China) containing wild-type 3′-UTR of NFIB (NFIB-WT) or mutant 3′-UTR of NFIB (NFIB-MUT) were constructed. HEK293T cells were plated in 24-well plates at 20,000 cells per well. 24 hours later, we transfected the plasmid (0.5 mg) into cells and simultaneously transfected miR-495 mimic or mimic negative control (mimic-NC). The activity of Luciferase was detected using Dual-Glo® Luciferase Assay System.

### Statistical Analysis

Statistical analysis was performed using Statistical Product and Service Solutions (SPSS) 22.0 software (IBM, Armonk, NY, USA). Data were represented as mean ± Standard Deviation (SD). The *t*-test was used for analyzing measurement data. Differences between two groups were analyzed by using the Student's *t*-test. Comparison between multiple groups was done using One-way ANOVA test followed by Post-Hoc Test (Least Significant Difference). $p<0.05$ indicated the significant difference.

**Table I.** Real time PCR primers.

| Gene name | Forward (5′>3′) | Reverse (5′>3′) |
|---|---|---|
| miR-495 | GGGAAACAAACATGGTGCA | GAGAGGAGAGGAAGAGGGAA |
| U6 | CTCGCTTCGGCAGCACA | AACGCTTCACGAATTTGCGT |

RT-PCR, quantitative reverse-transcription polymerase chain reaction.

## Results

### *Hypoxia Induced Apoptosis and Up-Regulated MiR-495 in H9c2 Cells*

H9c2 cell viability after hypoxia for 8 hours, 10 hours and 12 hours were detected by MTT assay. In the case of 10 hours of hypoxia, the viability of H9c2 cells decreased by about 50%, so in the subsequent experiments, 10 hours of hypoxia was used as the condition for establishing a cell model of MI (Figure 1A). Hypoxia significantly induced an increase in LDH release from H9c2 cells (Figure 1B). In addition, the treatment of hypoxia dramatically decreased Bcl-2 expression, but markedly increased the Bax expression and the ratio of Cleaved Caspase-3 / total Caspase-3 (C-Caspase-3 / T-Caspase-3) (Figure 1C). Moreover, hypoxia treatment can greatly increase the apoptosis rate of H9c2 cells (Figure 1D). Through RT-PCR, we found that compared with the con-

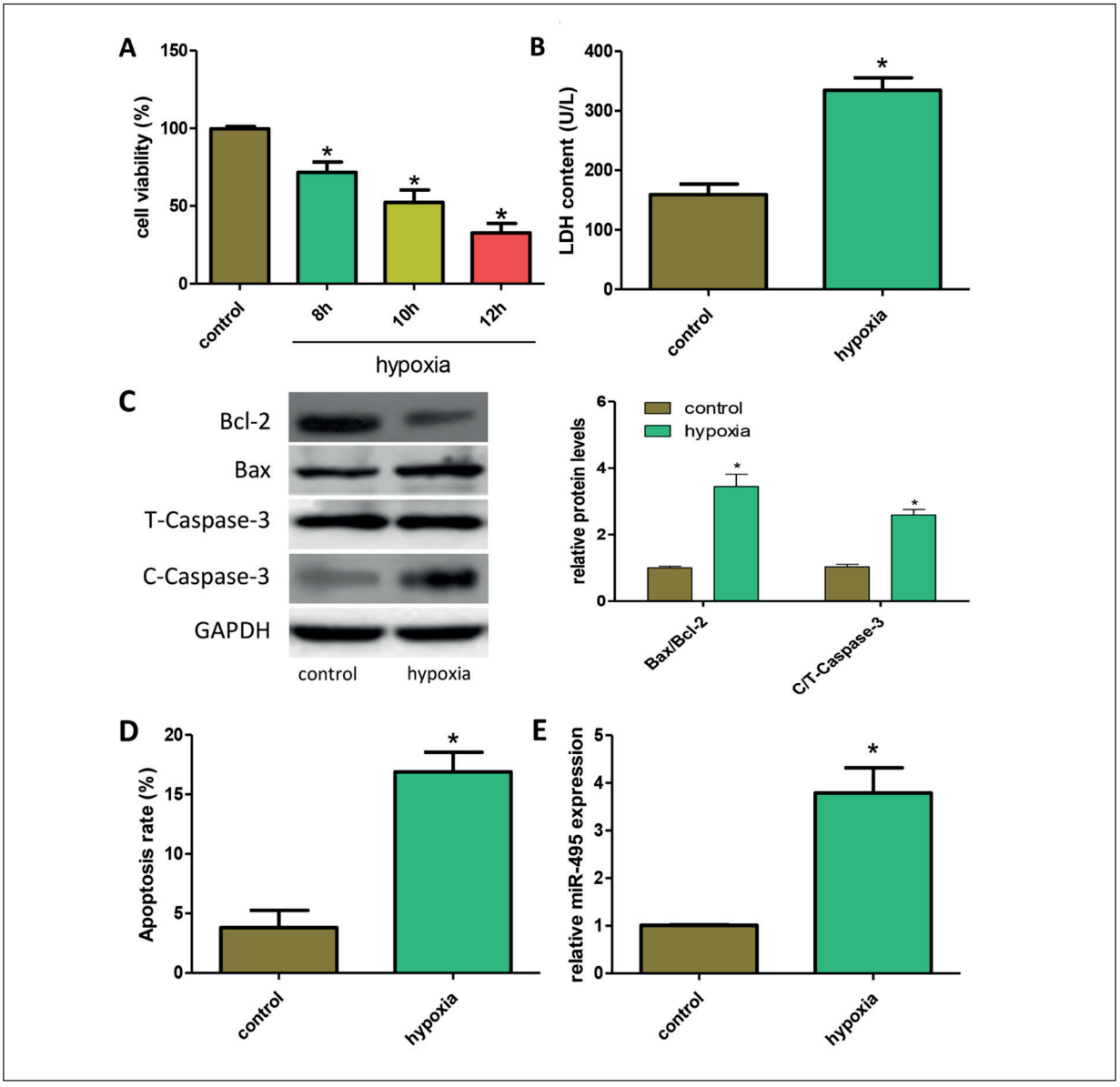


**Figure 1.** Hypoxia induced apoptosis and up-regulated miR-495 in H9c2 cells. **A,** Viability of H9c2 cells treated with different periods of hypoxia was measured using MTT assay ("*" $p<0.05$ *vs.* control, n = 3). **B,** LDH contents in cell supernatant ("*" $p<0.05$ *vs.* control, n = 3). **C,** Expression levels of apoptosis-related proteins (Bcl-2, Bax, Caspase-3 and Cleaved Caspase-3) were detected by Western blot ("*" $p<0.05$ *vs.* control, n=3). **D,** Hypoxia treatment induced apoptosis of H9c2 cells ("*" $p<0.05$ *vs.* control, n=3). **E,** MiR-495 expression decreased in H9c2 cells treated with hypoxia MiR-495 expression was normalized to U6 expression. ("*" $p<0.05$ *vs.* control, n=3).

trol group, miR-495 expression in the hypoxic group was noticeably increased (Figure 1E). The above results indicated that hypoxia treatment could induce the apoptosis of H9c2 cells and up-regulate miR-495 expression.

### Down-Regulation of MiR-495 Inhibitted Hypoxia-Induced Apoptosis of H9c2 Cells

Transfection of miR-495 inhibitor greatly inhibited miR-495 expression in H9c2 cells (Figure 2A). Down-regulation of miR-495 reversed the hypoxia-induced decrease in the viability of H9c2 cells (Figure 2B). In addition, down-regulation of miR-495 markedly reduced the contents of LDH in the cell supernatant (Figure 2C). Compared with the hypoxia + NC group, Bcl-2 expression in the hypoxia+inhibitor group increased significantly, and Bax expression and the ratio of C-Caspase-3 / T-Caspase-3 decreased observably (Figure 2D). Moreover, the results of flow cytometry proved that the inhibition of miR-495 can inhibit hypoxia-induced apoptosis of H9c2 cells (Figure 2E). Similarly, the results of TUNEL staining showed that silencing of miR-495 significantly reduced the number of TUNEL-positive cells (Figure 2F). These results demonstrated that down-regulation of miR-495 inhibited hypoxia-induced apoptosis of H9c2 cells.

### MiR-495 Directly Targets NFIB

Through TargetScan software, NFIB was found may have a binding site with miR-495 (Figure 3A). Through Western blot, we found that down-regulation of miR-495 remarkably inhibited NFIB expression (Figure 3B). Most importantly, luciferase activity assay showed that overexpression of miR-495 remarkably inhibits the luciferase activity in NFIB-WT group but not in NFIB-MUT group, which proved that NFIB has a binding site with miR-495 (Figure 3C).

### Down-Regulation of MiR-495 Inhibited Hypoxia-Induced Apoptosis of H9c2 Cells Via Targeting NFIB

SiR-NFIB or siR-NC and miR-495 inhibitor were co-transfected into H9c2 cells, and the cells were treated with hypoxia. Compared with the +siR-NC group, the expression of NFIB and Bcl-2 in the +siR-NFIB group was markedly reduced, while Bax expression and the ratio of C-Caspase-3 / T-Caspase-3 were greatly increased (Figure 4A). In addition, knockdown of NFIB markedly increased hypoxia-induced LDH release in H9c2 cells (Figure 4B). Moreover, silencing NFIB also increased the apoptosis rate of H9c2 cells, as evidenced by flow cytometry and TUNEL staining (Figure 4C and 4D). In sum, these results indicated that down-regulation of miR-495 inhibited hypoxia-induced apoptosis of H9c2 cells by targeting NFIB.

## Discussion

AMI refers to an acute occlusion of the coronary arteries, which leads to a rapid reduction or interruption of coronary blood flow caused by myocardial ischemia, hypoxia and necrosis. Because AMI is one of the main causes of death in humans worldwide, researching effective methods to treat myocardial infarction is one of the common problems faced by basic cardiovascular researchers and clinicians. As we all know, when MI occurs, the blood flow is interrupted, which will eventually cause the death of myocardial cells and the remodeling of the ventricle. Myocardial remodeling is a very important process of heart failure, including myocardial hypertrophy, myocardial cell apoptosis, and myocardial fibrosis[11-13]. Because myocardial cells lack the ability to regenerate, chronic heart failure is often one of the undesirable consequences of myocardial injury[14]. Therefore, when AMI occurs, it is important to preserve a certain number of cardiomyocytes to survive, which is very important for maintaining cardiac function, preventing cardiac remodeling, and improving the prognosis of patients.

Cell death is defined as the irreversible cell membrane integrity is destroyed and cytoplasm is lost[15]. The death of myocardial cells is a significant feature of MI[16]. At present, the death of mammalian cells is divided into three categories according to morphology: necrosis, apoptosis and autophagic cell death[17]. Apoptosis, also known as type II cell death. At present, there are many studies on the molecular mechanism of apoptosis, mainly divided into two mechanisms: one is exogenous apoptosis (also known as death receptor pathway), and the other is endogenous apoptosis (the mitochondrial pathway)[18]. Exogenous apoptosis is mediated by death receptors to form a death-inducing signal complex (DISC), which in turn activates caspase-8, and activated caspase-8 eventually activates caspase-3 to induce apoptosis[19]. Unlike exogenous apoptosis, endogenous apoptosis activates multiple signaling pathways, including growth factors, oxidative stress, hypox-

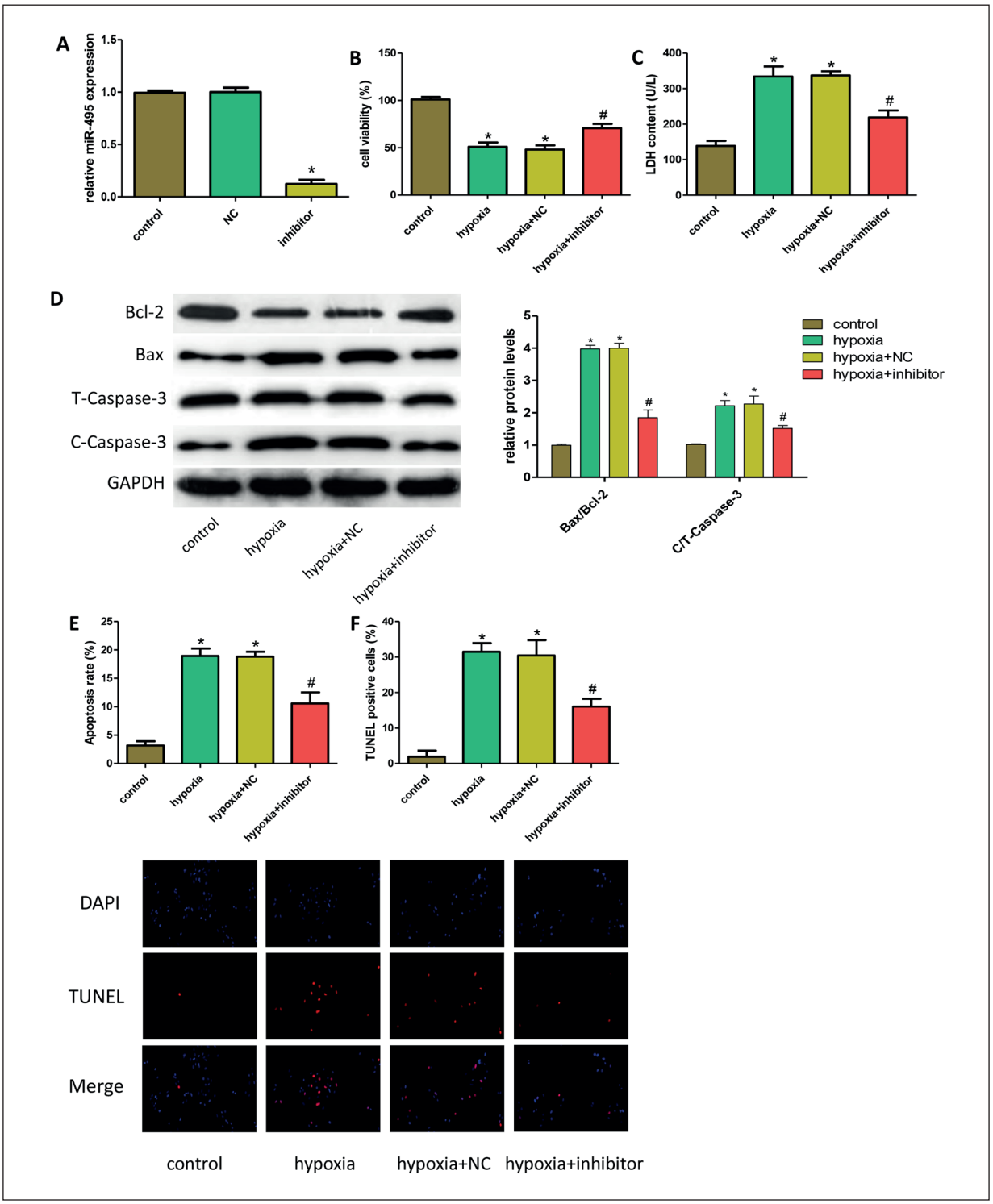


***Figure 2.*** Down-regulation of miR-495 inhibited hypoxia-induced apoptosis of H9c2 cells. **A,** Transfection of miR-495 inhibitor significantly inhibited the level of miR-495 in H9c2 cells ("$_{*}$" $p<0.05$ *vs.* NC, n=3). **B,** Viability of H9c2 cells was measured using MTT assay ("$_{*}$" $p<0.05$ *vs.* control, "$_{\#}$" $p<0.05$ *vs.* hypoxia+NC, n=3). **C,** LDH contents in cell supernatant ("$_{*}$" $p<0.05$ *vs.* control, "$_{\#}$" $p<0.05$ *vs.* hypoxia+NC, n=3). **D,** Expression levels of apoptosis-related proteins (Bcl-2, Bax, Caspase-3 and Cleaved Caspase-3) were detected by Western blot ("$_{*}$" $p<0.05$ *vs.* control, "$_{\#}$" $p<0.05$ *vs.* hypoxia+NC, n=3). **E,** The apoptosis rate of H9c2 cells was detected by flow cytometry ("$_{*}$" $p<0.05$ *vs.* control, "$_{\#}$" $p<0.05$ *vs.* hypoxia+NC, n=3). **F,** Results of TUNEL staining of H9c2 cells in each group (magnification: 200×) ("$_{*}$" $p<0.05$ *vs.* control, "$_{\#}$" $p<0.05$ *vs.* hypoxia+NC, n=3).

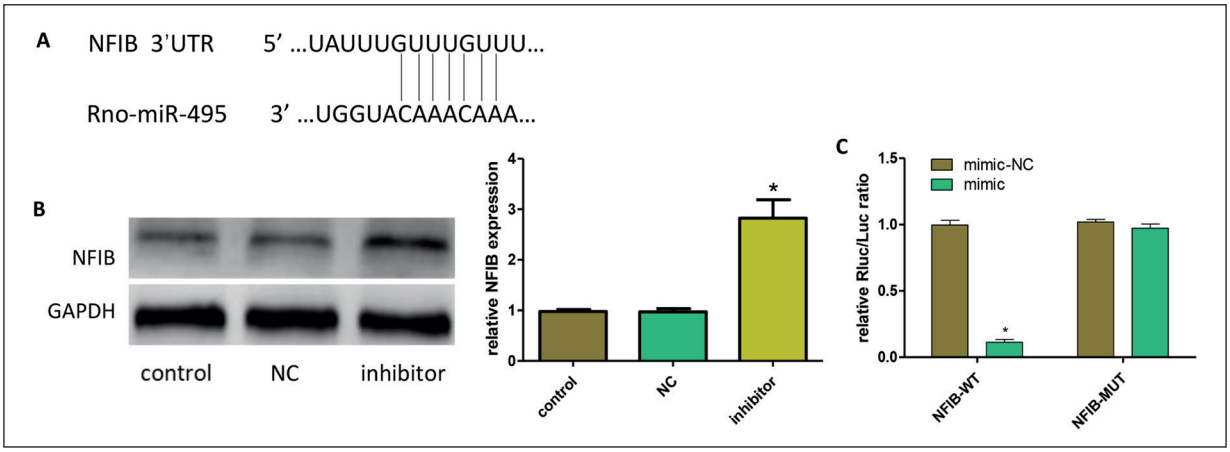


**Figure 3.** MiR-495 directly targets NFIB. **A,** Binding site predicted by the TargetScan database. **B,** Western blot showed the expression of NFIB ("*" $p<0.05$ *vs.* NC, n=3). **C,** MiR-495 overexpression significantly decreased the relative luciferase activity in NFIB-WT group, but did not decrease the relative luciferase activity in NFIB-MUT group ("*" $p<0.05$ *vs.* mimic-NC, n = 3).

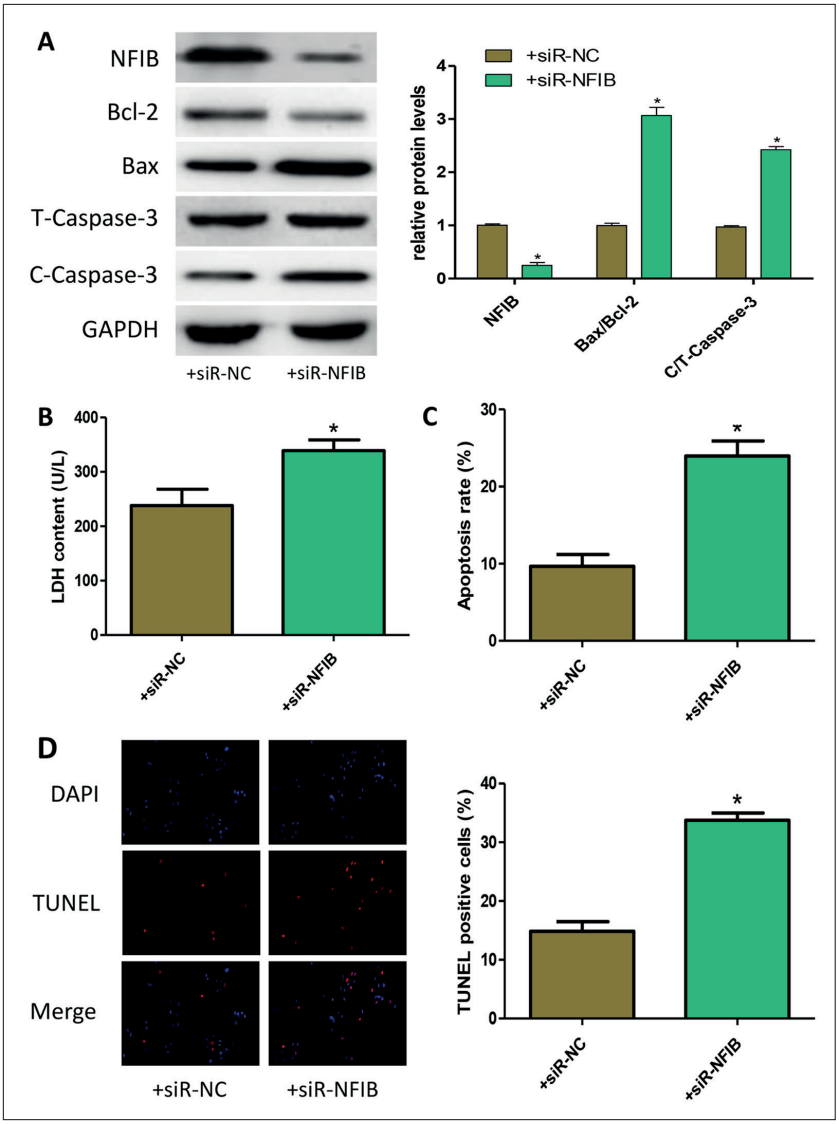


**Figure 4.** Down-regulation of miR-495 inhibited hypoxia-induced apoptosis of H9c2 cells via targeting NFIB. **A,** Expression levels of proteins (NFIB, Bcl-2, Bax, Caspase-3 and Cleaved Caspase-3) were detected by Western blot ("*" $p<0.05$ *vs.* +siR-NC, n=3). **B,** LDH contents in cell supernatant ("*" $p<0.05$ *vs.* +siR-NC, n=3). **C,** The apoptosis rate of H9c2 cells was detected by flow cytometry ("*" $p<0.05$ *vs.* +siR-NC, n=3). **D,** Results of TUNEL staining of H9c2 cells (magnification: 200×) ("*" $p<0.05$ *vs.* +siR-NC, n=3).

ia, and DNA damage[20,21]. When the endogenous apoptosis pathway is activated, the first activated pro-apoptotic proteins Bax and Bak induce cytochrome c (cyto-c) release. After cyto-c enters the cytoplasm from mitochondria, it activates Apafl and caspase-9, and the activated caspase-9 further cleaves caspase-3 to eventually trigger apoptosis[22,23]. Although exogenous and endogenous apoptosis pathways are two different signaling pathways, they are also interrelated.

So far, some papers have reported that miRNAs are involved in the regulation of myocardial apoptosis after MI, such as miR-145, miR-214, miR-488-3p, etc[24-26]. In this article, we induced apoptosis of H9c2 cells by hypoxia treatment, and revealed that miR-495 expression was increased in hypoxia-treated H9c2 cells. Down-regulation of miR-495 significantly inhibited the apoptosis of H9c2 cells. Through the Luciferase reporter gene experiment, we further proved that NFIB is the target gene of miR-495. Subsequent rescue experiments proved that the anti-apoptotic effect produced by down-regulation of miR-495 was achieved by targeting NFIB.

## Conclusions

In the present study, we successfully constructed an *in vitro* model of MI using hypoxia treatment, and, for the first time, we revealed the increased expression of miR-495 in the *in vitro* model of MI. In addition, miR-495 silencing significantly inhibited hypoxia-induced cardiomyocyte apoptosis. Further, the rescue experiments demonstrated that miR-495 silencing inhibited hypoxia-induced cardiomyocyte apoptosis in a NFIB-dependent manner. In sum, miR-495 expression was elevated in hypoxia-treated H9c2 cells. Downregulating miR-495 significantly inhibited myocardial apoptosis by targeting NFIB.

### Conflict of Interest

The Authors declare that they have no conflict of interests.

## References


1) Anderson JL, Morrow DA. Acute myocardial infarction. N Engl J Med 2017; 376: 2053-2064.
2) Proctor P, Leesar MA, Chatterjee A. Thrombolytic therapy in the current ERA: myocardial infarction and beyond. Curr Pharm Des 2018; 24: 414-426.
3) Boateng S, Sanborn T. Acute myocardial infarction. Dis Mon 2013; 59: 83-96.
4) Dai X, Kaul P, Smith SJ, Stouffer GA. Predictors, treatment, and outcomes of STEMI occurring in hospitalized patients. Nat Rev Cardiol 2016; 13: 148-154.
5) Lu TX, Rothenberg ME. MicroRNA. J Allergy Clin Immunol 2018; 141: 1202-1207.
6) Chistiakov DA, Orekhov AN, Bobryshev YV. Cardiac-specific miRNA in cardiogenesis, heart function, and cardiac pathology (with focus on myocardial infarction). J Mol Cell Cardiol 2016; 94: 107-121.
7) Wojciechowska A, Braniewska A, Kozar-Kaminska K. MicroRNA in cardiovascular biology and disease. Adv Clin Exp Med 2017; 26: 865-874.
8) Bernardo BC, Ooi JY, Lin RC, McMullen JR. miRNA therapeutics: a new class of drugs with potential therapeutic applications in the heart. Future Med Chem 2015; 7: 1771-1792.
9) Chen G, Xie Y. miR-495 inhibits proliferation, migration, and invasion and induces apoptosis via inhibiting PBX3 in melanoma cells. Onco Targets Ther 2018; 11: 1909-1920.
10) Liang J, Huang W, Cai W, Wang L, Guo L, Paul C, Yu XY, Wang Y. Inhibition of microRNA-495 enhances therapeutic angiogenesis of human induced pluripotent stem cells. Stem Cells 2017; 35: 337-350.
11) van Berlo JH, Maillet M, Molkentin JD. Signaling effectors underlying pathologic growth and remodeling of the heart. J Clin Invest 2013; 123: 37-45.
12) Koshman YE, Patel N, Chu M, Iyengar R, Kim T, Ersahin C, Lewis W, Heroux A, Samarel AM. Regulation of connective tissue growth factor gene expression and fibrosis in human heart failure. J Card Fail 2013; 19: 283-294.
13) Chen C, Li R, Ross RS, Manso AM. Integrins and integrin-related proteins in cardiac fibrosis. J Mol Cell Cardiol 2016; 93: 162-174.
14) Bergmann O, Bhardwaj RD, Bernard S, Zdunek S, Barnabe-Heider F, Walsh S, Zupicich J, Alkass K, Buchholz BA, Druid H, Jovinge S, Frisen J. Evidence for cardiomyocyte renewal in humans. Science 2009; 324: 98-102.
15) Kroemer G, Galluzzi L, Vandenabeele P, Abrams J, Alnemri ES, Baehrecke EH, Blagosklonny MV, El-Deiry WS, Golstein P, Green DR, Hengartner M, Knight RA, Kumar S, Lipton SA, Malorni W, Nunez G, Peter ME, Tschopp J, Yuan J, Piacentini M, Zhivotovsky B, Melino G. Classification of cell death: recommendations of the Nomenclature Committee on Cell Death 2009. Cell Death Differ 2009; 16: 3-11.
16) Whelan RS, Kaplinskiy V, Kitsis RN. Cell death in the pathogenesis of heart disease: mechanisms and significance. Annu Rev Physiol 2010; 72: 19-44.
17) Nikoletopoulou V, Markaki M, Palikaras K, Tavernarakis N. Crosstalk between apoptosis, necro-

sis and autophagy. Biochim Biophys Acta 2013; 1833: 3448-3459.

18) Youle RJ, Strasser A. The BCL-2 protein family: opposing activities that mediate cell death. Nat Rev Mol Cell Biol 2008; 9: 47-59.

19) Ashkenazi A, Dixit VM. Death receptors: signaling and modulation. Science 1998; 281: 1305-1308.

20) Kaufmann T, Tai L, Ekert PG, Huang DC, Norris F, Lindemann RK, Johnstone RW, Dixit VM, Strasser A. The BH3-only protein bid is dispensable for DNA damage- and replicative stress-induced apoptosis or cell-cycle arrest. Cell 2007; 129: 423-433.

21) Orogo AM, Gustafsson AB. Cell death in the myocardium: my heart won't go on. IUBMB Life 2013; 65: 651-656.

22) Levine B, Sinha S, Kroemer G. Bcl-2 family members: dual regulators of apoptosis and autophagy. Autophagy 2008; 4: 600-606.

23) Pagliari LJ, Kuwana T, Bonzon C, Newmeyer DD, Tu S, Beere HM, Green DR. The multidomain proapoptotic molecules Bax and Bak are directly activated by heat. Proc Natl Acad Sci U S A 2005; 102: 17975-17980.

24) Zheng HF, Sun J, Zou ZY, Zhang Y, Hou GY. MiRNA-488-3p suppresses acute myocardial infarction-induced cardiomyocyte apoptosis via targeting ZNF791. Eur Rev Med Pharmacol Sci 2019; 23: 4932-4939.

25) Yin Y, Lv L, Wang W. Expression of miRNA-214 in the sera of elderly patients with acute myocardial infarction and its effect on cardiomyocyte apoptosis. Exp Ther Med 2019; 17: 4657-4662.

26) Yan L, Guo N, Cao Y, Zeng S, Wang J, Lv F, Wang Y, Cao X. miRNA145 inhibits myocardial infarctioninduced apoptosis through autophagy via Akt3/mTOR signaling pathway in vitro and in vivo. Int J Mol Med 2018; 42: 1537-1547.